



ISSN 2314-5609  
Nuclear Sciences Scientific Journal  
8, 213- 230  
2019  
<http://www.ssnma.com>

## URANIUM REMOVAL FROM NITRATE SOLUTION BY CATION EXCHANGE RESIN (AMBERLITE IR 120), ADSORPTION AND KINETIC CHARACTERISTICS

EBRAHIM A. GAWAD  
*Nuclear Materials Authority, Egypt*

### ABSTRACT

The present work aims to study the adsorption behavior of uranium ions from nitrate solutions using the strong acid cation exchange Amberlite IR120 resin. Batch shaking sorption experiments are carried out to evaluate the performance of the studied resin in the uranium adsorption. The adsorption parameters including contact time, pH, initial uranium concentration and temperature have been optimized. The physical parameters including the adsorption kinetics, the isotherm models and the thermodynamic data have also been determined to describe the nature of the uranium adsorption by the investigated resin. The modelled data has been found to agree with both the exothermic pseudo first order reaction and the Langmuir isotherm. The applied procedure was used for uranium ions removal from scrub and raffinate liquors.

### INTRODUCTION

Solid-liquid extraction of uranium from its resources has proved to be more advantageous in view of the total insolubility of the applied solid in the aqueous phase, its low rate of physical degradation besides its high sorption capacity as well as its good flexibility and kinetic properties (Technical Reports Series No. 359, 1993, and Donat et al., 2009). In this respect, ion exchange methods are widely used for the hydrometallurgical recovery of uranium from acidic leached mineral ore bodies (Merritt et al., 1971).

The earliest uranium separation process had been based on the development of ion exchange resins containing anion exchange functional groups. This is due to the fact that uranium ions in the sulfate leach liquors are generally present as anionic sulfate complexes

and can thus be selectively extracted leaving the other impurities in cationic species. Consequently, the most commonly used resins in uranium recovery processes were strong base anion exchange resins containing quaternary ammonium groups (Streat et al., 1987). Based on this fact, many researches have reported the application of several anion exchange resins upon the sulfate leach liquors such as Amberlite IRA-400 (Guettaf et al., 2009, and Khawassek 2014), Amberlite IRA-402 (Abdel Aal 2014), AMn resin (Mirjial 2007), Amberlite IRA-425 (Abd El-Ghany et al., 1994), Dowex-IX8 (Barnes et al., 1974), Ambersep 920U Cl, and Amberlite IR-118H (Cheira 2014, Liberti et al., 1983, and Kilislioglu et al., 2003) for uranium recovery from its solutions. On the contrary, Sadeek et al. was used amine functionalized glycidyl methacrylate to extract uranium species in the nitrate media (Sadeek

et al., 2014). Who-ever, Othman et al., 2010 studied the optimum extraction conditions of beryllium on flow-through fixed bed reactor of Amberlite IR-120 (Othman, 2010).

The current paper is focused on the uptake behavior of uranium (VI) from nitric acid media by solid phase extraction using the strong base Amberlite IR120 resin. The parameters affect the rate of uranium adsorption from aqueous nitric acid solution as an indication of the performance of Amberlite IR120 resin is studied. In the meantime, the optimum loading conditions were interpreted via sorption kinetic and adsorption isotherm modeling.

Modeling (or idealization) of processes has now become standard operating procedure to bridge the gap between classical work and modern applications. By being acquainted with the mathematical model of a process it is possible to control and maintain it at an optimal level, provide maximal yield of the product, and obtain the product at a minimal cost. In convent, one often meets mathematical models in engineering practice that are not linear either by their regression coefficients or their independent variables. Nonlinearity by regression coefficients, however, is a heavier problem and it is nowadays solved by iterative procedure helped by some software such as MATLAB, ASPEN, and POLYMATH etc. (Gawad, 2009).

Non-linear relations greatly rely on graphical representations. On the other hand, linear fitting is often used to estimate the characteristics of many systems due to the simplicity of the relation. Various linear models lead to certain offset of estimated values. This fact is proved by statistical calculations. Therefore, it is much more reliable to find out precise coefficients using non-linear methods. On applying linear models, it is recommended to take into consideration the approximate values rather than exact data set (Subramanyam et al., 2009). The careful non-linear formulation is an important pathway for better model simulation.

## EXPERIMENTAL

### Materials and Methods

All reagents used were of analytical reagent grade. Uranyl nitrate [ $\text{UO}_2(\text{NO}_3)_2$ ] was supplied from Riedel–deHaen. The uranyl nitrate synthetic solutions were prepared by dissolving the exact amount of uranyl nitrate in distilled water. The working Amberlite 120 IR resin (AIR) was purchased from Dow Chemical Company. The properties and structural formula was represented in appendix (1). The liquid solution used in this study from scrub and raffinate liquors was collected from solvent extraction unit at Nuclear Materials Authority, Egypt. The quantitative analysis of uranium was achieved spectrophotometrically by UV single beam multi-cells positions spectrophotometer model SP-8001, Metretech Inc., version 1.02 using Arsenazo III [Marczenko et al 2000] at pH 2 (Rohwer et al., 1997) and ascertained by an oxidimetric titration against ammonium metavanadate method using N-phenyl anthranilic acid indicator (Sigma-Aldrich), (Davies et al., 1964–Mathew, 2009).

### Equilibrium Studies

To study the effect of controlling variables on the adsorption process, a series of batch experiments were performed using the standard uranium nitrate solution. It involves contact time, pH, initial uranium concentration and the effect of adsorbent dose. From the obtained results, Langmuir, Freundlich, Redlich–Peterson as well as Brunauer–Emmett–Teller (BET) isotherms were determined.

### Analytical Procedure

The adsorption experiments were performed by shaking 0.05 g AIR resin with 10 mL of the uranium nitrate synthetic solution (of 100 mg/L initial uranium concentration) using a magnetic stirrer. The adsorbed amounts of uranium species were calculated by the difference between its equilibrium and initial concentrations. The amount of uranium

adsorbed on the solid phase  $q_e$  (mg/g) was calculated using the following relation:

$$q_e = (C_o - C_e) \times \frac{V}{m} \quad (1)$$

where  $C_o$  and  $C_e$  are the initial and equilibrium concentrations of the uranium (mg/L), respectively,  $V$  is the volume of the aqueous phase (L), and  $m$  is the weight of the AIR resin used (g). The adsorption percent of ions from the aqueous phase was determined from the following relation:

$$\text{Uranium adsorption \%} = \frac{C_o - C_e}{C_o} \times 100 \quad (2)$$

The distribution coefficient ( $K_d$ ) of uranium between the aqueous bulk phase and the solid phase was calculated from the following relation:

$$K_d = \frac{C_o - C_e}{C_e} \times \frac{V}{m} \quad (3)$$

**Equilibration Calculation**

All uranium speciation in this study were performed with Hydra-MEDUSA, a chemi-

cal equilibrium calculation program [Puigdomenech I. HYDRA].

**RESULTS AND DISCUSSION**

**Effect of Contact Time**

The impact of changing the contact time from 5 to 45 was examined through a series of experiments by contacting a fixed weight of AIR resin (0.05 g) with a uranium solution (10 mL) having a concentration of 100 mg/L and pH 1 at temperature (15, 20, 25, 30, 35 and 40 °C), (Fig.1).

As shown, the uranium adsorption efficiency attained about 75% for 25 minutes at temperature 15 °C while it reached to 80% at 45 min. By increasing the contact time from 30 to 45 minutes, the uranium adsorption efficiencies approximately remained constant. Consequently, 30 minutes contact time could be selected as the suitable time. We can notice the reverse effect of temperature on the adsorption.

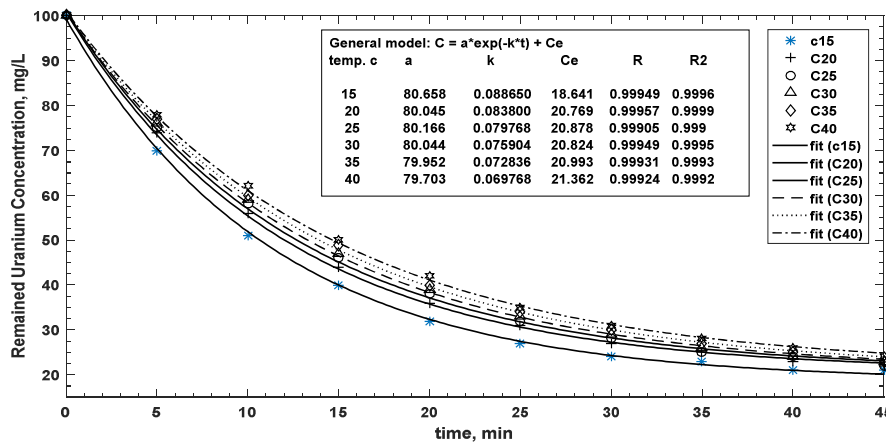


Fig.1:Effect of contact time upon the uranium adsorption percent on the AIR resin: intrinsic rate of the reaction (absolute uptake  $dc/dt = (m/V)(dq/dt)$ ) at various temperatures (Resin weight= 0.05 g, volume = 10 ml, pH = 1, U conc. =100mg/L)

### Effect of pH

The effect of pH on uranium adsorption efficiency on AIR from nitrate solution was examined by contacting a fixed weight of the AIR (0.05g) with a portion (10 mL) of uranium standard solution of 100 mg/L at 25°C for 30 minutes contacting time. The examined pH ranged from 0.2 to 9.0. The obtained results plotted on Fig.(2) indicates that maximum uranium adsorption efficiency was obtained at pH 1.0. A decrease in uranium adsorption efficiency at pH less than 1 is related to the competition of H<sup>+</sup> adsorption (by increasing acidity). Increasing the solution pH from 1.0 to 4.0, followed by a slight decrease in the

uranium adsorption as a result of the predominance of uranium cation species ( $\text{UO}_2(\text{NO}_3)^+$ , and  $\text{UO}_2^{2+}$ ). Further increase in solution pH more than 4, a significant decrease in uranium adsorption efficiency was obtained due to disappear of the latter uranium cation species as shown on Fig.(3). According to the experiment of initial pH 1.0 the possible coordination mechanism for the interaction among  $\text{UO}_2\text{NO}_3^+$ ,  $\text{UO}_2^{2+}$ , and AIR resin may be as follows;



and

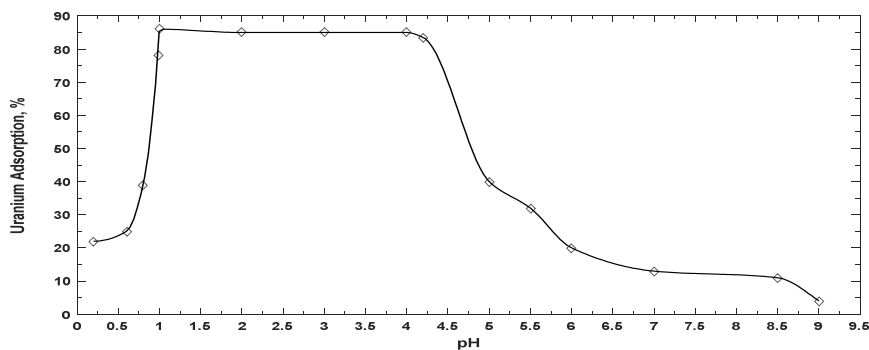


Fig.2:Effect of solution pH on the adsorption percentage of uranium onto the AIR ( $[\text{UO}_2^{2+}] = 100 \text{ mg/L}$ , AIR = 0.05 g, aqueuse volume = 10 mL, 30 min, 25 °C)

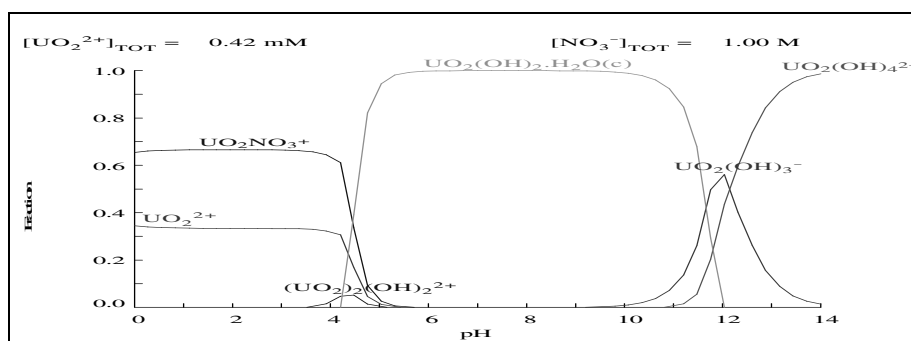


Fig. 3:Uranium species calculated by Hydra/Medusa, ( $[\text{UO}_2^{2+}] = 100 \text{ mg/L} = 0.42 \text{ mM}$ ,  $T=25 \text{ }^\circ\text{C}$  in 1 M  $\text{HNO}_3$ ).

### Effect of Agitation Speed

The effect of the agitation speed was studied in the range between 50–300 rpm at room temperature for 30 min. The adsorption percent of uranium increased to 80% as the stirring rate increased to 150 rpm then remained constant by increasing agitation speed. Therefore, the preferred speed was 150 rpm which was used for all the subsequent tests. The results are shown on Fig.(4).

### Effect of Initial Uranium Concentration

A series of experiments were performed to investigate the influence of initial uranium concentration upon the adsorption efficiency onto Amberlite IR120 resin. The studied initial uranium concentrations ranged from 10

up to 6000 mg/L were contacted with a fixed weight (0.05 g) of the studied resin. The obtained results illustrated on Fig.(5) showed that the adsorption capacity increased with increasing the initial uranium concentration up to 3000 ppm. Therefore, the determined adsorption capacity was found about 106.1 mg uranium/g resin.

### Effect of Resin Amount

A series of adsorption experiments was performed using different adsorbent doses ranging from 0.01 up to 0.2 g resin/L. The influence of adsorbent amount on the uptake of uranium was represented on Fig(6). The results revealed that the adsorption efficiency increases from 77.8 to 83.87% with increasing adsorbent amount from 0.01 to 0.05g resin/L.

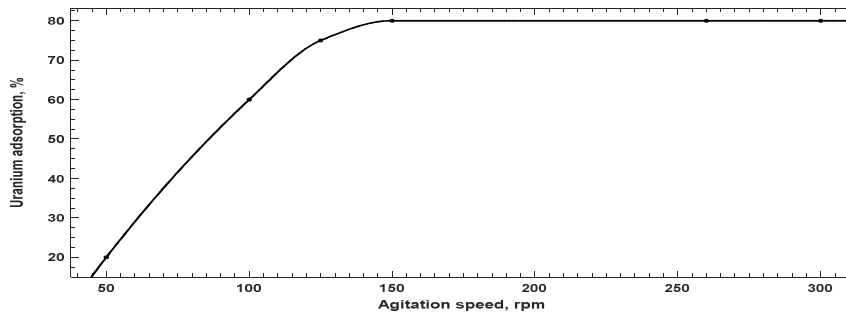


Fig.4:Effect of Agitation speed on the adsorption of uranium onto the Amberlite IR120 (U conc. =100 mg/L, resin weight = 0.05 g, pH=1, volume=10 ml, 20 min, 25 °C)

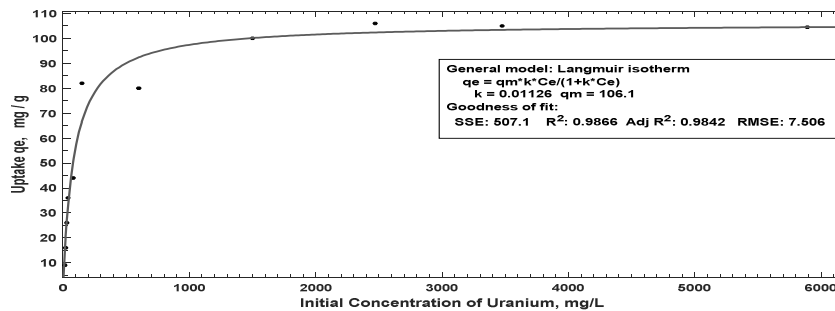


Fig.5: Effect of initial uranium concentrations on uranium uptake onto the Amberlite IR120 resin (Resin weight = 0.05 g, volume = 10 ml, pH=1, 30 min, 25 °C)

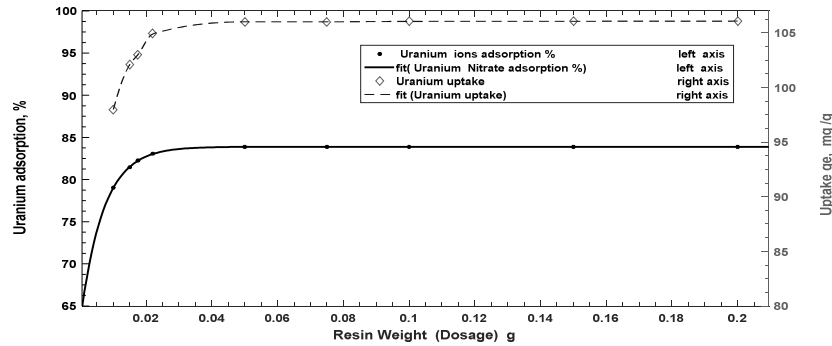


Fig.6:Effect of adsorbent dose upon uranium adsorption % and uptake onto Amberlite IR120

Further increasing of the AIR resin amount the active sites become more plentiful than the available uranium ions in the solution. Consequently, the adsorptive capacity of adsorbent available was not fully utilized at a higher adsorbent amount. Based on the latter, 0.05 g AIR resin/L is preferred as the usable adsorbent amount.

#### Adsorption Isotherm

A number of common adsorption isotherm models were considered to fit the attained isotherm data under the equilibrium adsorption of the AIR resin. Langmuir, Brunauer–Emmett–Teller (BET), Redlich–Peterson and Freundlich isotherms models were applied. Previously, uranium uptake was represented as mg/g as shown on Figs. (5&6) while herein, the representation took place as eq/L to compare the results with the producer-provided data.

#### Langmuir isotherm

Langmuir model supposes that, the adsorption occurs uniformly on the active sites of the sorbent, and once a sorbate occupies a site, no further sorption can take place at this site (Sheng et al., 2016- Li et al., 2014). Thus, the Langmuir model is given by the following equation:

$$q_e = q_{\max} \frac{kC_e}{1 + kC_e} \quad (4)$$

where:  $q_{\max}$  and  $k$ , the Langmuir constants, are the saturated monolayer sorption capacity and the sorption equilibrium constant, respectively.

A non-linear simulation of equation (4) produced the corresponding parameters are presented on Fig. (7) and Table (1). The values of  $q_{\max}$  0.891 eq/L (106.065 mg/g) and  $k$  0.0113 L/mg, they are closely match with the obtained values  $R^2 = 0.986$ . It means that Langmuir is anticipated as the representative isotherm for this system. The applicability of this isotherm was further analyzed by a dimensionless equilibrium parameter,  $R_L$  (ratio of unused adsorbent capacity to the maximum adsorbent capacity) in appendix (2).

#### Freundlich isotherm

The Freundlich model stipulates that the ratio of solute adsorbed to the solute concentration is a function of the solution. The empirical model was shown to be consistent with exponential distribution of active centers, characteristic of heterogeneous surfaces (Manes et al., 1969). The amount of solute adsorbed at equilibrium,  $q_e$ , is related to the concentration of solute in the solution,  $C_e$ , by the following:

$$q_e = K_F C_e^{1/n} \quad (5)$$

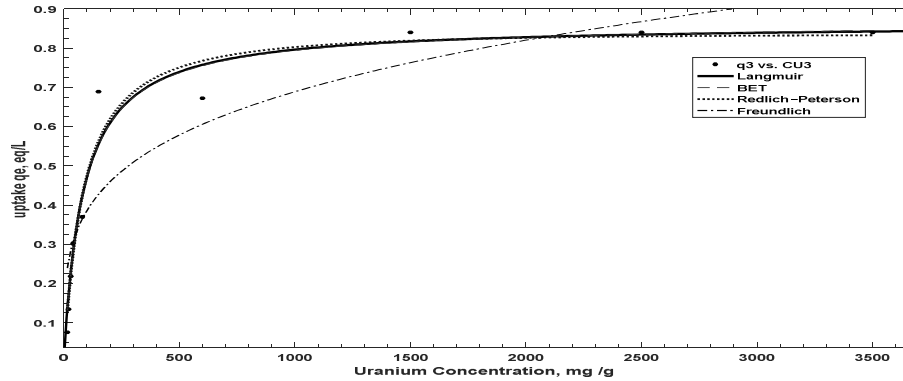


Fig.7: Isotherms plot for adsorption of uranium onto AIR resin

Table 1: Langmuir, BET, Redlich–Peterson and Freundlich parameters for uranium adsorption on to AIR resin

Isotherm	Parameters	SSE *	R <sup>2</sup>	adj R <sup>2</sup>	RMSE **
Langmuir	$q_{max} = 0.8913$ eq/L = (106.0647 mg/g) $k = 0.01126$ L/mg $CBET = 4.249e+05$ $Cs = 3.649e+07$ mg/g	0.01425	0.986	0.9837	0.04513
BET	$qs = 0.8747$ eq/L (104.0775) mg/g note $CBET / Cs = 0.011644286$	0.01149	0.986	0.984	0.04052
Redlich–Peterson	$aR = 0.01289$ L/mg $g = 0.9867$ L/g $kR = 0.01038$ L/g or $q_m = 0.8746$ eq/L $k = 0.01154$ L/mg $n = 0.9974$ factor	0.0139	0.98644	0.98422	0.04456
Freundlich	$kf = 0.1157$ L/mg $n = 0.2622$ factor	0.1262	0.8641	0.8471	0.1256

\*SSE: Sum of Squares Due to Error    \*\* RMSE: Root Mean Squared Error    For both SSE and RMSE: A value closer to 0 indicates that the model has a smaller random error component, and that the fit will be more useful for prediction

where  $K_f$  and  $n$  are the Freundlich constants, which represent sorption capacity and sorption intensity, respectively. Freundlich constants of this work are given in Table (1),  $R^2 = 0.864$  which reveal that, Freundlich isotherm model can't represent this system.

**Redlich–Peterson isotherm model**

Redlich–Peterson isotherm (Redlich et al., 1959-Prasad et al., 2009) is a hybrid isotherm

featuring both Langmuir and Freundlich isotherms, which incorporate three parameters into an empirical equation. The model has a linear dependence on concentration in the numerator and an exponential function in the denominator to represent adsorption equilibria over a wide concentration range, that can be applied either. Typically, a minimization procedure is adopted in solving the equations by maximizing the correlation coefficient between the experimental data points and theo-

retical model predictions. Redlich–Peterson isotherm is given by the following equation (7):

$$q_e = \frac{k_R C_e}{(1 + a_R C_e^g)} \quad (6)$$

or as Langmuir family form

$$q_e = q_m \frac{k C_e}{(1 + k C_e^n)} \quad (7)$$

Where  $k_R$ ,  $a_R$  and  $g$  are the Redlich–Peterson which represent saturated sorption capacity and the sorption equilibrium constant and sorption intensity respectively.

A non-linear simulation of equation (6 and 7) produced the corresponding parameters as seen on Fig(7). Redlich–Peterson constants are given in Table (1) which mean that this isotherm is a mathematical function;  $q_m$  0.87 eq/L (104.07 mg/g) and almost represent the practical uptake value 106.06 as shown previously.

#### Brunauer–Emmett–Teller (BET)

Brunauer–Emmett–Teller (BET) (Ng et al., 2002, Bruanuer et al 1938, and–Foo et al., 2010) isotherm is a theoretical equation, most widely applied in the gas–solid equilibrium systems. It was developed to derive multi-layer adsorption systems with relative pressure ranges from 0.05 to 0.30 corresponding to a monolayer coverage lying between 0.50 and 1.50. Its extinction model related to liquid–solid interface is exhibited as the following equation (8):

$$q_e = \frac{q_s C_{BET} C_e}{(C_s - C_e)[1 + (C_{BET} - 1)(C_e / C_s)]} \quad (8)$$

where  $C_{BET}$ ,  $C_s$ ,  $q_s$  and  $q_e$  are the BET adsorption isotherm (L/mg), adsorbate monolayer saturation concentration (mg/L), theoretical isotherm saturation capacity (mg/g) and equilibrium adsorption capacity (mg/g), respectively.

Practically  $q_s$  and  $(C_{BET} / C_s)$  are analogy to  $q_{max}$  and  $k$  in Langmuir model. BET constants are given in Table (1) which mean that as mentioned in Redlich–Peterson isotherm this iso-

therm is a mathematical function;  $q_m$  0.87 eq/L (104.07 mg/g). It almost represents the real uptake value of U, 106.06.

From Table (1):Although, there is a stiff competition among the first three isotherms but Langmuir constants are more matching with the practical values. Therefore, Langmuir is satisfy to represent this system. The  $q_{max}$  provided by the producer is ~1.8eq/L while the calculated  $q_{max}$  for the three isotherms is ~0.9 it means intermediate affinity to uranium. A comparison of the adsorption capacity of AIR resin with some other sorbents is provided in Table (2).

#### Adsorption Modeling and Kinetics

The data are fitted with pseudo  $n^{th}$ - order rate equation which can be derived as follow for any pseudo  $n$  order:

$$\frac{dq}{dt} = k (q_e - q_t)^n \quad (9)$$

Which on separation and integration yields

$$q_t = q_e - (q_e^{(1-n)} + (k (n-1) t))^{(1/(1-n))} \quad (10)$$

or by introducing Arrhenius relation in (10) and rearrange we obtain:

$$(q_e - q_t)^{(1-n)} + q_e^{(1-n)} = (n-1)tk_0 e^{(\frac{AE}{RT})} \quad (11)$$

$$q_t = q_e - \left( q_e^{(1-n)} + \left( (n-1)tk_0 e^{(\frac{AE}{RT})} \right) \right)^{(1/(1-n))} \quad (12)$$

Fig (8) simulates eq. (10) and declares that –in a workable approximation–the pseudo first order is the predominant kinetic model. Figure (9) shows the uptake– time relation of this heterogeneous system in analogy to pseudo reversible first order in homogeneous system. We can notice the compatibility of  $k$  values in Figs (8 & 1). The decreases in  $k$  values accompanying the increase in temperature indicate an exothermic reaction. Figures (9-11) represent general kinetic model, pseudo first order, and pseudo second order systems respectively in 3D using MATLAB. The representation of nonlinear models in 3D enabled process engi-

Table 2: The experimental capacity of AIR resin compared with the adsorption capacity of some resins and different solvent modified polymers

Type	q <sub>max</sub> (mg/g)	Ref.
polyethyleniminephenylphosphonamidic acid	39.66	Abderrahimet al 2009
N-dimethyl-N,N-dibutylmalonamide functionalized polymer	18.78	Ansari et al 2009
polymer	12.33	Metilda et al 2005
succinic acid impregnated amberlite XAD-4 gel-amide	28.98	Venkatesan et al 2004
gel-benzamide	18.64	
natural clinoptilolite zeolite	0.7	Camacho et al 2010
Ambersep 920U C1	51.2	Ferrah et al 2015
Lewatit TP 214	81.75	Cheira et al 2015
4-(2-Pyridylazo)resorcinol (PAR), Amberlite XAD-16	115.5	Rahmati et al 2012
Amberlite IRA-910	64.26	Ho et al 1999
Amberlite IRI20	106.065	Wazne et al 2003
		Present work

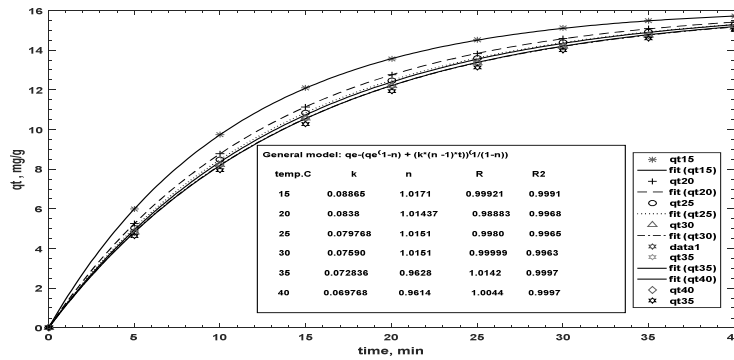


Fig.8: Determination of the Kinetic Model at various temperatures, (Resin weight = 0.05 g, volume = 10 ml, pH = 1, U conc. = 100 mg/L)

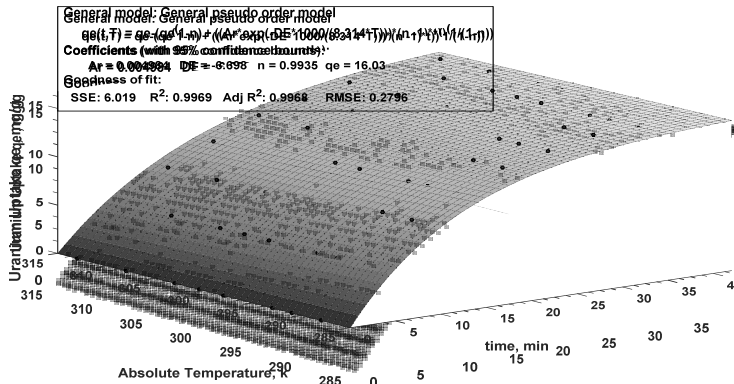


Fig.9: uptake–(time and temperature) dependency (general pseudo order system)

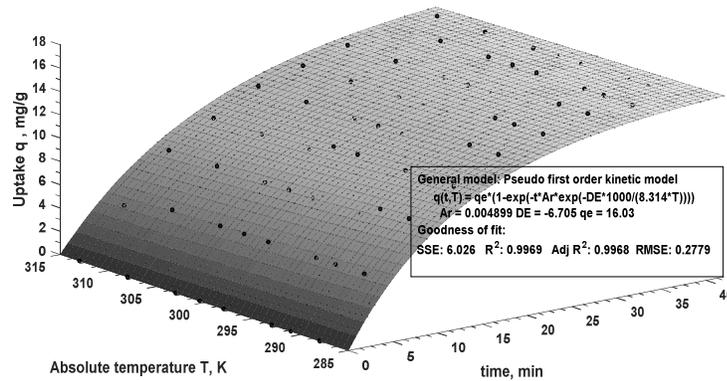


Fig.10: uptake–(time and temperature) dependency (pseudo 1st order system)

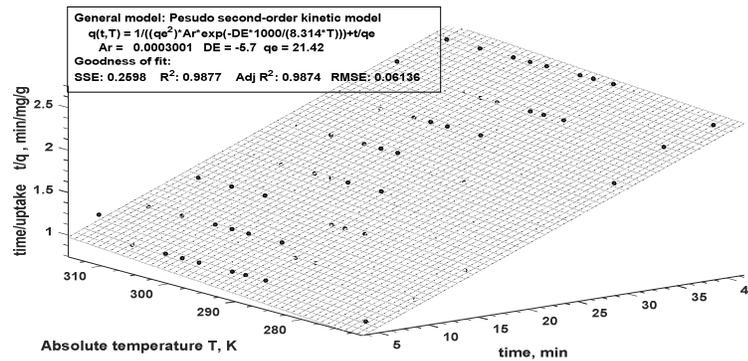


Fig.11: Determination of the pseudo second order kinetic model in 3D

neer to acquire many alternatives when facing any process shortage. In general it is a one of the good supports when making a decision.

The magnitude of activation energy gives information about the type of adsorption, which is physical or chemical adsorption. The physisorption processes usually have activation energies in the range of 0–40 kJ/mol, while higher activation energies (40–800 kJ/mol) suggest chemisorptions (Liu et al 2012, Li et al., 2012 and Ilaiyaraja et al., 2017). The obtained value of activation energy is less than 40 kJ/mol (6.698 kJ/mol for U(VI) indicates that physisorption of U(VI) onto AIR resin.

The calculated correlation coefficients are closer to unity for the pseudo first order kinetic model. The calculated equilibrium adsorption capacity ( $q_e$ ) is consistent with the experimental data. The obtained data featured in 3D Figs (9-11) show that the process can be approximated more satisfactorily by the pseudo first order as the predominant mechanism.

### Thermodynamic Characteristics

The thermodynamic parameters of the studied adsorption process have been determined for uranium adsorption upon AIR resin. Series of experiments were carried out

at various temperatures ranging from 15 to 45 °C. These parameters were calculated for this system using the following non-linear Van't Hoff equation:

$$K_d = e^{\left(\frac{-\Delta H}{RT} + \frac{\Delta S}{R}\right)} \quad (13)$$

To produce more adequate results we can represent the matrix of distribution coefficient  $K_d(t,T)$  as follow:

$$K_d(t,T) = k_d(t) e^{\left(\frac{-\Delta H}{RT} + \frac{\Delta S}{R}\right)} \quad (14)$$

We can simulate eq (14) in 3D using MATLAB as shown on Fig (12), where  $K_d$  (ml/g),  $\Delta H$  (KJ/mol),  $\Delta S$  (J/mol.K), T (Kelvin) and R (KJ/K.mol) are the distribution coefficient, the enthalpy, the entropy, the temperature in Kelvin and the molar gas constant, respectively.

The Gibbs free energy,  $\Delta G$  (KJ/mol), is calculated from the following equation:

$$\Delta G = \Delta H - T\Delta S \quad (15)$$

Also it can be calculated from the isotherm constant from equation (16):

$$\Delta G_{iso} = -RT \ln(k) \quad (16)$$

The calculated enthalpy change ( $\Delta H$ ) and the entropy change ( $\Delta S$ ) 5.628 KJ/mol and 53.24 J/mol, respectively. The negative value of  $\Delta H$  confirms the exothermic nature of adsorption process. The negative value of free energy of adsorption  $\Delta G$  confirms the feasi-

bility and spontaneous nature of adsorption process. Thus, the adsorption process was found to be exothermic and spontaneous. The negative value of  $\Delta S$  indicates a decrease in the randomness at the solid/solution interface during the sorption of uranium ions onto the sorbent. Randomness arises due to the destruction of hydration shell of U(VI) species prior to adsorption (Liu et al., 2012; Li et al., 2012; Ilaiyaraja et al., 2017 and Ingelezakis et al., 2006). Practically, by regarding to Figs (13&19) this system is limited to spontaneous regime as shown on Fig (13). The break-even point in the latter figure, indicates that the process of uranium adsorption can take place in reversible manner but the forward is the predominant till  $\sim 347$  °k ( $\sim 74$  °C).

### FT-IR Spectroscopy and Scan Electron Microscopy

FT-IR spectroscopy and SEM were employed to demonstrate the interactions between Amberlite IR120 resin and U(VI). The spectra of Amberlite IR120 resin before and after loading with U(VI) are presented on Fig (14). The FT-IR spectrums exhibited several peaks. The peak around  $3380 \text{ cm}^{-1}$  for strong band of the -OH stretching vibrations was observed for both situations. On the lower frequency side, the band at about  $2931 \text{ cm}^{-1}$  was related to the stretching vibrations of the ring

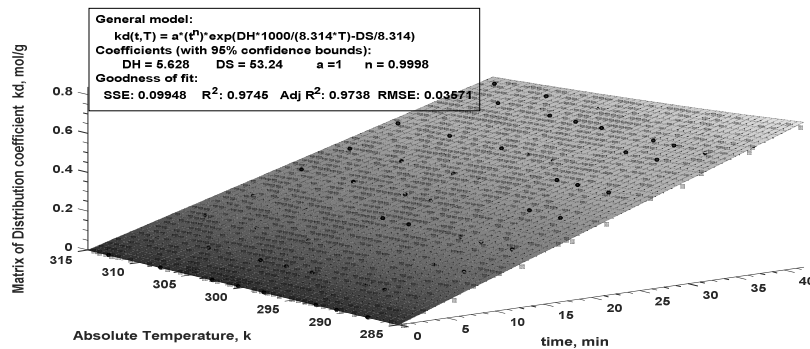


Fig. 12: Plot of  $K_d$  as a function of time and absolute temperature of uranium ions onto AIRresin (note that using DH and DS instead of  $\Delta H$  and  $\Delta S$ , respectively)

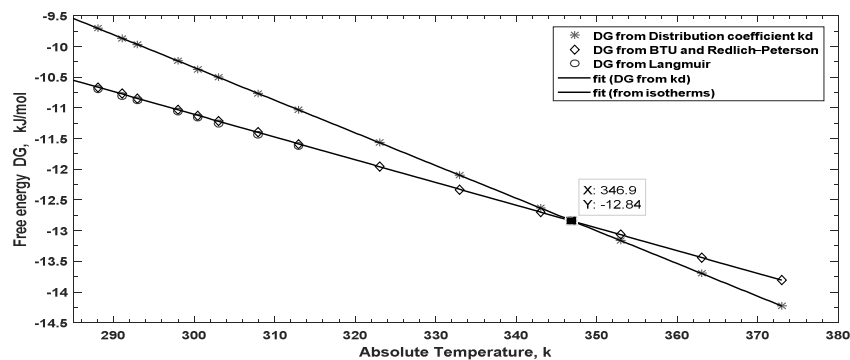


Fig.13: Break-even point of Free Energy (note that using DG instead of  $\Delta G$ )

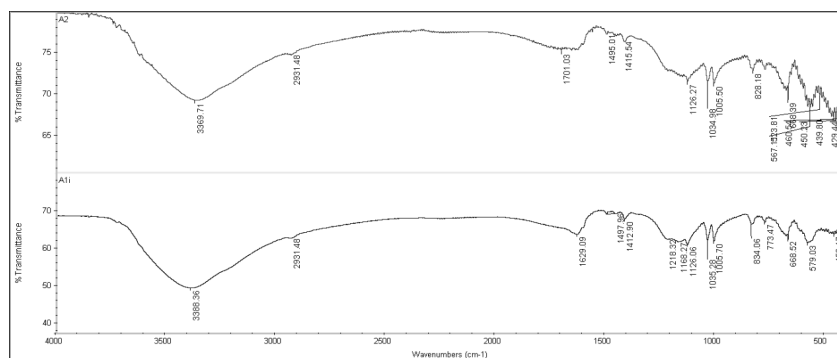


Fig.14: FT-IR spectrum of Amberlite IR120 resin before and after uranium adsorption

C-H bands of the resin (cross-linked polystyrene). The sharp peaks were found at  $1630\text{ cm}^{-1}$  (C=C skeletal vibration),  $1495\text{ cm}^{-1}$  (C-N vibration), and  $1415\text{ cm}^{-1}$  (O-H bending vibration). The ring C-C stretching and the scissoring of the methylene groups (bending  $-\text{CH}_2$ ) appeared at  $1495$  and  $1415\text{ cm}^{-1}$ . After the adsorption, the intensity of some bands changed and transmittance of peaks was relatively greater in the case of loaded resin with U(VI) most bands were shifted from  $10$ - $15\text{ cm}^{-1}$ , that actually, provided evidence of the interaction between U(VI) and the nitrogen atom of tertiary amine group in AIR resin as uranyl anion complex. A signal corresponding to the vibration of  $\text{O}=\text{U}=\text{O}$  at  $1218$  and  $1168$

$\text{cm}^{-1}$  was also observed, suggesting the uptake of U(VI) by studied resin (Abdien et al., 2016 and Abderrahim et al., 2009).

The SEM images of the AIR resin before and after U(VI) adsorption are shown on Figs (15-18), respectively. The images declare the difference between the surfaces of the AIR resin. Although a good uniformity and smooth surface was observed in the conventional resin, the surface after U(VI) adsorption was observed as a bright spherical spots on the resin beads. As can be seen from the results, a visible change of the surface morphology in the U(VI) adsorbed resin demonstrated that the sorption of U(VI) had taken place onto the AIR resin.

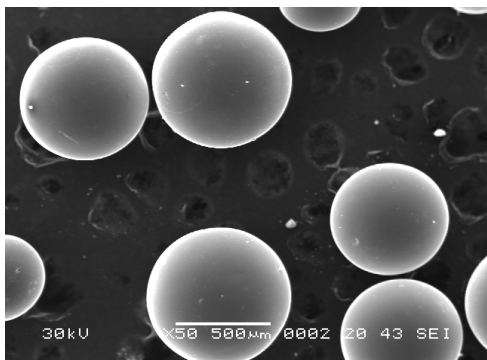


Fig.15:SEM micrograph of Amberlite IR120 resin before U(VI) adsorption

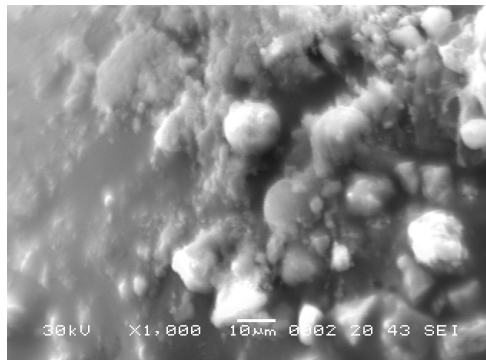


Fig.18:SEM micrograph of Amberlite IR120 resin after U(VI) adsorption

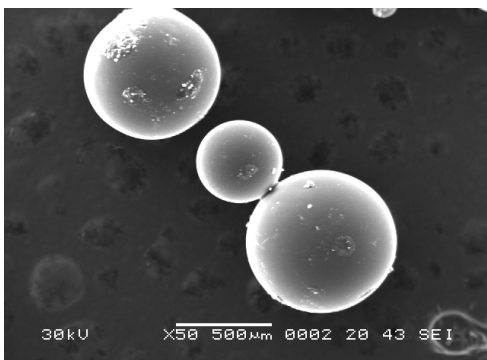


Fig.16:SEM micrograph of Amberlite IR120 resin after U(VI) adsorption

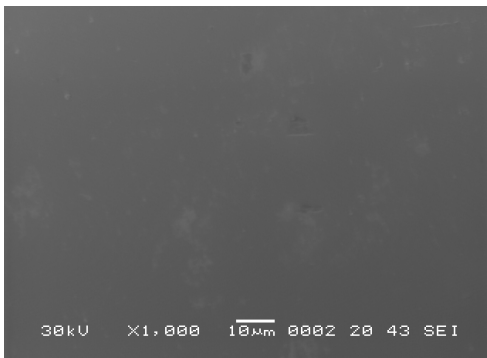


Fig.17:SEM micrograph of Amberlite IR120 resin before U(VI) adsorption

### Case study

The uranium removal and recovery from scrub and raffinate mixture collected from solvent extraction unit, Nuclear Materials Authority, Egypt was carried out. For this purpose (5batch) experiments were performed by contacting 0.496 g AIR with 550 mL of the studied liquor for 30 min. By calculating the accumulated loaded uranium it was found that about 66.533 mg U/g were adsorbed i.e. 62.73% of the theoretical capacity was realized. The decrease in the AIR capacity after contacting with the raffinate sample may be due to the competition among uranium and different ions in the studied sample (particularly Fe and Na). The chemical composition of the studied mixture before and after treatment is presented in Table (3). The adsorbed uranium has been eluted effectively from loaded AIR bed using 1.0 M nitric acid solution. Approximately, 58.49 mg uranium has been eluted with elution efficiency of 93.32%.

Figure (19) shows the simulation of the suggested representative model containing the factors affecting uranium removal from the real liquor.

### CONCLUSIONS

A commercial sorbent Amberlite IR120 (AIR) resin was tested for uranium adsorption.

The process was investigated as a function of various parameters such as contact time, pH, initial uranium concentration, resin dose and temperature. Equilibrium was attained after 30 min of contact time and the practical loading capacity was 106.1 mg U(VI)/g resin. The kinetics of uranium adsorption on AIR resin followed the pseudo first order rate reaction. The equilibrium isotherm for adsorption of the investigated metal ions had been modeled successfully using the Langmuir isotherm. The thermodynamic parameters confirmed the limited spontaneous, randomness and exothermic nature of physisorption. The optimized

affecting factors were applied for removal of uranium species from scrub and raffinate of uranium processing project.

## REFERENCES

- Abd El-Ghany, M.S.; Mahdy, M.A.; Abd El-Monem, N.M., and El-Hazek, N.T., 1994. Pilot Plant Studies on the Treatment of El-Atshan Uranium Ores, Eastern Desert. Egypt. 2<sup>nd</sup> Arab Conf. Peaceful Uses of Atomic Energy, AAEA, Cairo.
- Abdel Aal, M., 2014. Purification of Uranium Concentrate from Abo- Rushied Ore Material with Emphasize Upon Ion Exchange Technique, South Eastern Desert, Egypt, Fac. Sci., Ain Shams Univ.
- Abderrahim, O.; Didi, M.A., and Villemin, D., 2009. A new sorbent for uranium extraction polyethyleniminephenylphosphonamidic acid. J. Radioanal. Nucl. Chem. 279(1), 237–244.
- Abderrahim, O.; Didi, M.A., and Villemin, D., 2009. A new sorbent for uranium extraction polyethyleniminephenylphosphonamidic acid. J. Radioanal. Nucl. Chem. 279(1), 237–244.
- Abdien, H.G.; Cheira, M.F.; Abd-Elraheem, M.A.;

Table 3: Chemical composition of the studied scrub and raffinate mixture

Component	concentration, g/L		Removal, %
	before	after	
Mn	0.108	0.106	2
Fe	0.561	0.481	14.5
Mg	0.198	0.194	2
Ca	0.656	0.636	3
Na	1.238	1.139	8
AL	0.806	0.798	1
K	0.318	0.289	9
U	100 mg/L	40 mg/L	60

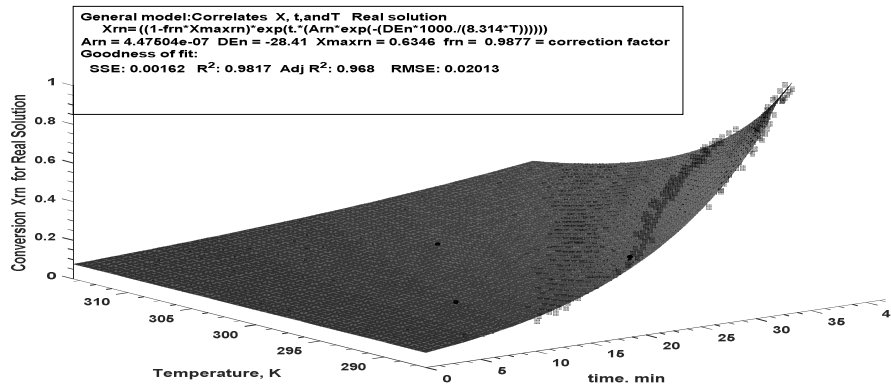


Fig.19: Pre-simulation of the governing factors affecting uranium removal using Amberlite IR 120 from scrub and raffinate liquor. (Note that using DE instead of  $\Delta E$ )

$X, t, T$  are, removal fraction, time, and absolute temperature, respectively  
 $X_{rn}$ : removal fraction at any  $t$ , and  $T$  while  $X_{maxrn}$ : maximum removal fraction  
 $A_{rn}$ : frequency factor and  $D_{En}$ : using it instead of  $\Delta E$  activation energy to avoid troubles

- El-Naser, T.A., and Zidan, I.H., 2016. Extraction and pre-concentration of uranium using activated carbon impregnated trioctyl phosphine oxide. *Elixir International J. Applied Chemistry* 100, 43462- 43469.
- Ansari, S.A.; Mohapatra, P.K., and Manchanda, V.K., 2009. A novel malonamide grafted polystyrene- divinyl benzene resin for extraction pre-concentration and separation of actinides. *J. Hazard Mater.* 161(2-3), 1323-1329.
- Barnes, C. D.; da Silva Neves R. A., and Streat M., 1974. Anion Exchange of Uranium from Aqueous Sulphuric Acid Solutions: Diffusion Kinetics. *J. appl. Chem. Biotechnol.* 24, 787-801.
- Bruanuer, S.; Emmett, P.H., and Teller, E., 1938. Adsorption of gases in multimolecular layers, *J. Am. Chem. Soc.* 60, 309–316.
- Camacho, LM.; Deng, S., and Parra RR., 2010. Uranium removal from groundwater by natural clinoptilolite zeolite: effects of pH and initial feed concentration. *J. Hazard Mater.*,175(1–3), 393–398.
- Cheira, M. F.; El-Didamony, A. M.; Mahmoud, K. F., and Atia, B. M., 2014. Equilibrium and Kinetic Characteristics of Uranium Recovery by the Strong Base Ambersep 920U Cl Resin, *IOSR-JAC*, 7(5), 32-40.
- Cheira, M.F., 2015. Synthesis of pyridylazo resorcinol – functionalized Amberlite XAD-16 and its characteristics for uranium recovery. *J. Environmental Chemical Engineering*, 3, 642–652.
- Davies, W., and Gray, W., 1964. A rapid and specific volumetric method for the precise determination of uranium using ferrous sulfate as a reductant. *Talanta*, 11, 1203-1211.
- Donat, R.; Cılgı, G.K.; Aytas, S., and Cetisl, H., 2009. Thermodynamics Parameters and Sorption of U (VI) on ACSD. *Radio analytical and Nuclear Chemistry*, 279, 271-280.
- Ferrah, N.; Abderrahim O., and Didi, M.A., 2015. Comparative Study of Cd<sup>2+</sup> Ions Sorption by Both Lewatit TP214 and Lewatit TP 208 Resins: Kinetic, Equilibrium and Thermodynamic Modelling. *Chemistry J.*, 5(1), 6-13.
- Foo, K.Y., and B.H. Hameed, 2010, Review Insights into the modeling of adsorption isotherm systems, *Chemical Engineering J.*, 156 (2010) 2–10].
- Gawad, E.A., 2009, recovery of some valuable ingredients from uranium effluents solutions, ph. Thesis, Fac.Eng., Alex. Univ.
- Guettaf, H.; Becis, A.; Ferhat, K.; Hanou, K.; Bouchiha, D.; Yakoubi K., and Ferrad, F., 2009. Concentration–Purification of Uranium from an Acid Leaching Solution. *Physics Procedia*, 2, 765–771.
- Ho, Y.S., and McKay, G., 1999. Pseudo-second order model for sorption processes, *Process Biochem.*, 34,451- 465.
- Ilaiyaraja, A.K.; Singha Deb.; Ponraju. D.; Musharaf. Sk., Ali, Venkatraman. B., 2017, Surface Engineering of PAMAM-SDB Chelating Resin with Diglycolamic Acid (DGA) Functional Group for Efficient Sorption of U(VI) and Th(IV) from Aqueous Medium
- Ingelezakis, V.J. ,and Pouloupoulos. S.G., 2006, Adsorption, Ion Exchange and Catalysis- design of operations and environmental applications, Elsevier
- Khawassek, Y.M., 2014. Production of Commercial Uranium Concentrate from El-Sela Shear Zone Mineralized Ore Material, South Eastern Desert- Egypt, at Inshas Pilot Plant Unit. *Nuclear Sciences Scientific J.*, 3, 169 – 179.
- Kilislioglu, A., Bilgin, B., 2003. Thermodynamic and kinetic investigations of uranium adsorption on amberlite IR-118H resin, *Applied Radiation and Isotopes*, 58, 155–160
- Li, L.; Ding, D.; Hu, N.; Fu, P.; Xin, X., and Wang, Y., 2014. Adsorption of U(VI) ions from low concentration uranium solution by thermally activated sodium feldspar. *J. Radioanal Nucl. Chem.*, 299, 681–690.
- Li, K.; Liu, Z.; Wen, T.; Chen, L., and Dong, Y., 2012.

- Sorption of radio cobalt(II) onto Ca-montmorillonite: Effect of contact time, solid content, pH, ionic strength and temperature, *J. Radio anal. Nucl. Chem.*, 292, 269–276.
- Liberti, L., and Helfferich, K., 1983. *Mass Transfer and Kinetics of Ion Exchange*, 1<sup>st</sup> Ed., Martinus Nijhoff Publishers, The Hague, Netherlands.
- Liu, Y, Lan, J, Zhao, Y, Yuan, L, Li, Z, Yuan, Y, Feng, Y, Chai, Z, Shi, W, 2012, A high efficient sorption of U(VI) from aqueous solution using amino-functionalized SBA-15, *J. Radio anal. Nucl. Chem.* 291 (2012) 803–810
- Manes, M., Hofer, L.J.E., 1969. Application of the Polanyi adsorption potential theory to adsorption from solution on activated carbon. *The Journal of Physical Chemistry* 73(3), 584–590.
- Marczenko, Z., Balcerzak, M., 2000. *Separation Preconcentration and Spectrophotometry in Inorganic Analysis*, Elsevier Science B.V., Amsterdam the Netherlands, p.521.
- Mathew, K.J., Mason, B., Morales, M.E., Narayann, U.I., 2009. Uranium assay determination using Davies and Gray titration: An overview and implementation of GUM uncertainty evaluation. *Radio analytical and Nuclear Chemistry* 282, 939-944.
- Merritt, R.C., 1971. *The Extractive Metallurgy of Uranium*, Colorado School of Mines Research Institute.
- Metilda P., Sanghamitra K., Mary Gladis, J., Naidu, G.R.K., Prasada Rao, T., 2005. Amberlite XAD-4 functionalized with succinic acid for the solid phase extractive preconcentration and separation of uranium (VI). *Talanta* 65(1), 192–200.
- Mirjial, K., Roshani, M., 2007. Resin-in-pulp method for uranium recovery from leached pulp of low grade uranium ore. *Journal of Hydrometallurgy* 85(2-4), 103-107.
- Ng, vJ.C.Y., Cheung, W.H., McKay, G., 2002. Equilibrium studies of the sorption of Cu(II) ions onto chitosan, *J. Colloid Interface Sci.* 255- 64–74.
- Othman, S. H., Salehb, M. M., Demerdash, M., El-Anadouli, B. E. 2010. Mathematical model: Retention of beryllium on flow-through fixed bed reactor of Amb-IR-120, *Chemical Engineering Journal* 156, 157–164.
- P. *Journal of Hazardous Materials* 328 (2017) 1–11
- Prasad, R.K., Srivastava, S.N., 2009. Sorption of distillery spent wash onto fly ash: kinetics and mass transfer studies, *Chem. Eng. J.* 146 (1) 90–97.
- Puigdomenech I. HYDRA (hydrochemical equilibrium-constant database) and MEDUSA (make equilibrium diagrams using sophisticated algorithms) programs, Royal Institute of Technology, Sweden. <https://www.kth.se/en/che/medusa/downloads-1.386254>
- Rahmati, A., Ghaemi, A., Samadfam, M., 2012. Kinetic and thermodynamic studies of uranium (VI) adsorption using Amberlite IRA-910 resin. *Ann. Nucl. Energy* 39, 42–48.
- Redlich, O., Peterson, D.L., 1959. A useful adsorption isotherm, *J. Phys. Chem.* 63 -1024–1026.
- Rohwer, H., Rheeder, N., Hosten, E., 1997. Interactions of uranium and thorium with arsenazoIII in an aqueous medium. *Anal Chim. Acta.* 341(2), 263–268.
- Sadeek, A. S., Abd El-Magied, M. O., El-Sayed, M. A., Amine M., M., 2014. Selective solid-phase extraction of U(VI) by amine functionalized glycidyl methacrylate, *Journal of Environmental Chemical Engineering* 2- 293–303.
- Sheng, L., Zhou, L., Huang, Z., Liu, Z., Chen, Q., Huang, G., Adesina, A.A., 2016. Facile synthesis of magnetic chitosan nano-particles functionalized with N/O-containing groups for efficient adsorption of U(VI) from aqueous solution. *J. Radioanal Nucl. Chem.* 310, 1361-1371.
- Streat M., Naden, D., 1987. *Ion Exchange in Uranium Extraction*, Critical Reports on Applied Chemistry Vol. 19, Ion Exchange and Separation Processes in Hydrometallurgy.

Subramanyam, B.; A. Das; autumn 2009; Linearized and non-linearized isotherm models comparative study on adsorption of aqueous phenol solution in soil, *Int. J. Environ. Sci. Tech.*, 6 (4), 633-640,

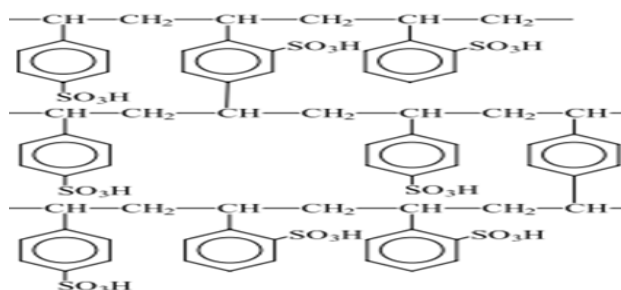
Technical Reports Series No. 359, 1993. Uranium Extraction Technology" International Atomic Energy Agency, Vienna,

Venkatesan, K., Sukumaran, V., Antony, M.P., Vasudeva Rao, P. R., 2004. Extraction of uranium by amine, amide and benzamide grafted covalently on silica gel. *J. Radioanal Nucl. Chem.* 260(3), 443-450.

Wazne, M., Korfiatis, G.P., Meng, X.G., 2003. Carbonate effects on hexavalent uranium adsorption by iron oxyhydroxide. *Environ. Sci. Technol.* 37,3619-3624.

### Appendix (1) Properties and formula of Amberlite IR 120

<b>Physical form</b>	<b>Amber spherical beads</b>
<b>Matrix</b>	<b>Styrene divinylbenzene copolymer</b>
<b>Functional group</b>	<b>Sulfonic acid</b>
<b>Ionic form as shipped</b>	<b>H+</b>
<b>Total exchange capacity</b>	<b>≥ 1.80 eq/L (H+ form)</b>
<b>Moisture holding capacity</b>	<b>53 to 58 % (H+ form)</b>
<b>Shipping weight</b>	<b>800 g/L</b>
<b>Particle size</b>	
<b>Uniformity coefficient</b>	<b>≤ 1.8</b>
<b>Harmonic mean size</b>	<b>0.620 to 0.830 mm</b> <b>&lt; 0.300 mm</b>
<b>Maximum reversible swelling</b>	<b>Na+ → H+ ≤ 11 %</b>



Structural formula of Amberlite IR 120

### Appendix (2)

The applicability of Langmuir adsorption isotherm was further analyzed by a dimensionless equilibrium parameter,  $R_L$  (ratio of unused adsorbent capacity to the maximum adsorbent capacity), (41-43) and is given by following equation

$$R_L = \frac{1}{(1+kC_0)}$$

The value of  $R_L$  indicates the nature of isotherm; unfavorable ( $R_L > 1$ ), linear ( $R_L = 1$ ), favorable ( $0 < R_L < 1$ ) or irreversible ( $R_L = 0$ ). The calculated  $R_L$  values fall within range 0 to 1 Fig. (App.1) indicating favorable adsorption of U(VI) on Amberlite IR 120 and the applicability of Langmuir isotherm. From this figure we can notice that, there are two adsorption paths in the relative rates =  $b/d = 11.625 \sim 1: 12$ .

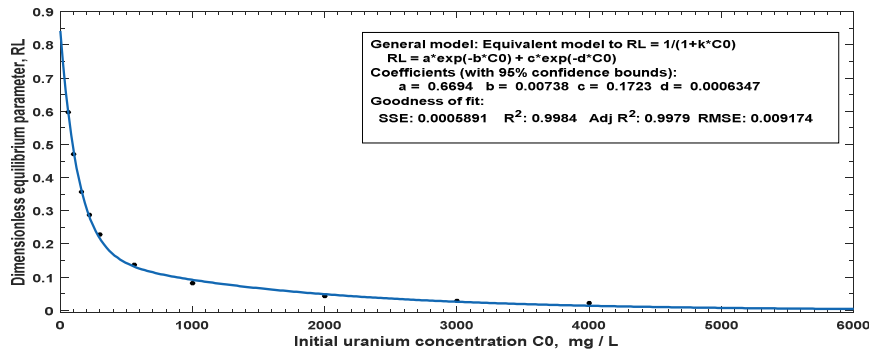


Fig (App.1): Relation between Dimensionless equilibrium parameter,  $R_L$  and initial uranium concentration for Amberlite IR 120

### ازالة اليورانيوم من محلول النترات باستخدام راتنج التبادل الكاتيوني (أمبرليت اي ار ١٢٠)، خواص وحركية الادمصاص

إبراهيم السيد أحمد عبد الجواد

يهدف هذا العمل إلى دراسة سلوك عملية ادمصاص أيونات اليورانيوم من محاليل النترات وذلك باستخدام راتنج التبادل الكاتيوني الحامضي القوى أمبرليت اي ار ١٢٠. أجريت تجارب دفعية لسبر أفضل الظروف للعوامل المؤثرة على عملية ادمصاص اليورانيوم. تشمل هذه العوامل وقت التلامس، والتركيز الأولي لليورانيوم، ورقم الأس الهيدروجيني للمحلول، وسرعة التقليب و حرارة العملية. علي الجانب الآخر تمت معالجة العوامل الفيزيائية والتي تشمل حركية الادمصاص ونموذج الايزوثيرم وثيرموديناميكية العملية وذلك لوصف طبيعة عملية الادمصاص لليورانيوم علس سطح الراتنج المستخدم. حيث تبين بعد دراسة النماذج أن عملية الادمصاص تتوافق مع تفاعل الرتبة الأولى المستتر والطارد للحرارة وكذلك ايزوثيرم لانجمير. وقد تم تطبيق منهجية الدراسة لإزالة أيونات اليورانيوم من خليط مجمع من محاليل الشطف والمحاليل المتبقية.